Segregation in a monolayer of magnetic spheres

Justin Stambaugh,[1] Zachary Smith,[4] Edward Ott,[1,3] and Wolfgang Losert[1,2,*]
[1]*Institute for Research in Electronics and Applied Physics and Department of Physics, University of Maryland, College Park, Maryland 20742, USA*
[2]*Institute for Physical Science and Technology, University of Maryland, College Park, Maryland 20742, USA*
[3]*Department of Electrical and Computer Engineering, University of Maryland, College Park, Maryland 20742, USA*
[4]*Department of Physics, Colorado School of Mines, Golden, Colorado 80401, USA*
(Received 2 April 2004; published 21 September 2004)

Segregation and pattern formation is investigated for binary mixtures of granular magnetic spheres in a vertically vibrated monolayer. The spheres, all of equal mass and size, have a maximum surface magnetic field B induced by encased cylindrical magnetic cores of length l. For binary mixtures of particles with equal l but different B, we find that the particles spontaneously segregate when driven. For fixed vibration frequency, the segregation rate increases roughly linearly with driving acceleration over the amplitudes investigated. For systems of fixed particle number density, the rate of segregation also decreases as the volume fraction of "strong" (high B) particles increases. We find that segregation also occurs in binary mixtures of particles with equal B, but different l. Finally, using a simple model of spheres with dipolar and higher magnetic moments, we show that the observed segregation phenomena occur in conjunction with a decrease in magnetic energy.

DOI: 10.1103/PhysRevE.70.031304 PACS number(s): 45.70.Mg, 61.30.Gd, 64.75.+g, 75.70.Ak

I. INTRODUCTION

Segregation in binary mixtures of excited granular material is a widely observed phenomenon [1]. Segregation due to differences in size [2–4], shape [5,6], density, and particle surface properties [3] has been observed to occur under various circumstances. In particular, there is significant current interest in the segregation and mixing of wet granular mixtures as an example of segregation among mutually attractive particles [3,4]. In granular systems, the addition of attractive forces between particles has been observed to both cause and prevent segregation under different circumstances [3]. Recent observations have also been made on pattern formation in systems of dry magnetic spheres, as an investigation of an anisotropically attractive granular material [7,8]. Blair and Kudrolli [8] found that, in a vertically vibrated two-dimensional (2D) mixture of magnetic and nonmagnetic granular spheres, the magnetic spheres can self-organize and cluster, depending on the volume fraction of magnetic particles and on the relative strength of the magnetic dipole-dipole interaction to the external vibration amplitude. In our earlier work [7], we showed that the shape of the magnetic field also influences into what pattern the beads self-assemble.

Pattern formation in other two-dimensional systems of dipolar particles has been investigated using many experimental and theoretical approaches [9]. Patterns have been observed experimentally in micrometer- to millimeter-sized magnetic particles suspended on the surface of a liquid [10–13], in a magnetic fluid containing nonmagnetic particles [12,14], at the atomic scale in thin magnetic films [15], and in Monte Carlo simulations of dipolar hard spheres [13,16–18]. Studies of biological systems also suggest that dipole-dipole interactions between proteins may play an important role in such phenomena as microtubule formation [19] and pattern formation in a lipid monolayer [20]. In addition to the previous work on vertically vibrated magnetic granular spheres [7,8], several groups have investigated vertically vibrated monolayers of unmagnetized granular particles [21–23]. However, the behavior of binary systems of granular matter that differs only in the shape or strength of the interaction potential, to our knowledge, has not been investigated. We present evidence that systems of vertically vibrated magnetic spheres of equal mass, size, and surface properties can segregate due only to differences in the particles' magnetic field strengths. We also show that magnetic spheres of equal magnetic field strength can segregate due only to differences in the field shape.

II. EXPERIMENTAL SETUP

The magnetic particles used were cylindrical permanent magnets securely encased in spherical hard plastic shells. Particles were constructed to have differently colored northern and southern hemispheres so that dipole orientations could be discerned. Figure 1 is a schematic of our magnetic particles. We investigate particles encasing magnetic cores of three types which we call "weak," "strong," and "long" magnets. The properties of all particles are shown in Table I. The weak particles have nearly identical shape, size, and mass as the strong particles, with the only relevant differing property being their relative magnetic strengths (measured as the maximum magnetic field on the surface of an isolated sphere). The strong and long particles have comparable magnetic strengths and are nearly identical in shape, size, and mass, with the only relevant differing property being their magnetic core shapes, i.e., their magnetic field shapes. The strong and weak magnets were encapsulated with nonmag-

*Electronic address: wlosert@glue.umd.edu; http://www.ipr.umd.edu/granular/dipolar/

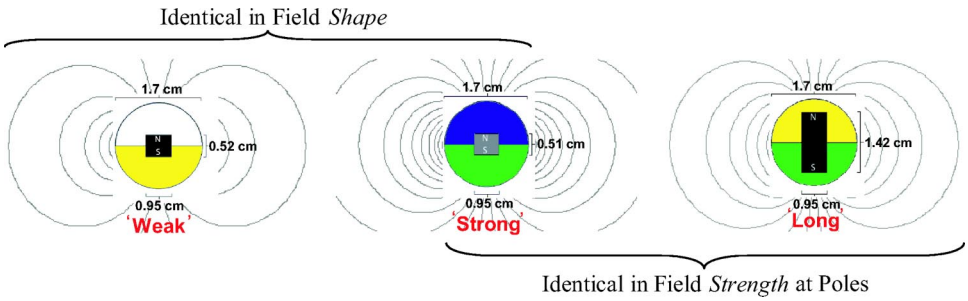

FIG. 1. (Color online) A general schematic of the magnetic particles used, together with a qualitative illustration of their respective magnetic field lines (obtained using VIZIMAG software).

netic filler of appropriate size and mass so that the magnets were centrally located and the finished particles were identical in mass.

A horizontal cylindrical container with a diameter 17.5 times a particle diameter and a height of 1.7 particle diameters was constructed with a Delrin bottom and a rigid transparent acrylic top (for imaging). A mixture of two types of particles was placed in the container so that the particles were well mixed, i.e., there were relatively small numbers of like-particle contacts. The system was then sinusoidally vibrated vertically at 30 Hz using an electromagnetic shaker. The use of vertical vibration as a means of inputting random energy into our granular system allows for our results to be compared qualitatively with earlier work on vertically vibrated magnetic granular systems [7,8]. The maximum strength of the magnetic field from the shaker at the inner container surface was 23.1 G at zero acceleration amplitude, although at typical acceleration amplitudes the rms magnetic field strength was of order 1 G. No noticeable effect due to any external magnetic field from the shaker was observed. The acceleration amplitude a was varied from $4g$ to $10g$ (where g is the acceleration of gravity) and was measured using an accelerometer. The system was imaged from above at a rate of 1 Hz with a 1280×1024 pixel color camera.

III. RESULTS

As an example of the observed patterns, Fig. 2(a) shows the mixed initial state of 88 weak and 23 strong particles. The initial state was made to have a low number of like-particle contacts. Figure 2(b) is the final state of the system in Fig. 2(a) after being shaken at $9.0g$ for 300 s. The final configuration [Fig. 2(b)] is highly segregated, with all strong blue/green (dark/dark in gray scale) particles in two dense clumps, and the weak white/yellow (light/light in gray scale) particles forming a loose, branching network pattern. The evolution of this system as shown in Figs. 2(a) and 2(b) indicates that systems of otherwise identical magnetic spheres can segregate due solely to differences in magnetic field strength.

A mixed initial state of 51 strong blue/green, and 59 long yellow/green (light/dark in gray scale) particles is shown in Fig. 3(a). After 300 s of excitation at $9.6g$, the system evolves into the configuration shown in Fig. 3(b). The final state [Fig. 3(b)] is well segregated, with the strong particles having a tendency toward hexagonal-close packed (hcp) clumps, and the long particles in long unbranched chains. The strong particles roughly tend toward hcp clumps while the long particles form long, unbranching chains as a consequence of their differences in magnetic field shape, as has been remarked upon earlier in a study of pattern formation in monodisperse 2D systems of magnetic spheres [7]. As evidenced in Figs. 3(a) and 3(b), systems of otherwise identical magnetic spheres can segregate due solely to differences in magnetic field shape.

For further analysis, we track the positions, 3D dipole orientations, and particle types of all particles during our experiments. To quantitify the segregation in each system, we designed a program that finds all particle-particle contacts in every image. The program identifies particles as "in contact" if the centers of the particles are within $9/8$ particle diameters of each other. We tested different cutoff values and found that our results do not qualitatively depend on the cutoff. We then define a segregation parameter for each image,

$$S = \frac{C_{AA}}{C_{AA}+C_{AB}} + \frac{C_{BB}}{C_{BB}+C_{AB}}, \tag{1}$$

where C_{ij} is the total number of "contacts" between particles of type i and particles of type j in the image (A and B are particle type labels). This segregation measure has the advantages of symmetry under interchange of particle type and equal weighting of the segregation of each particle type. $0 \leqslant S \leqslant 2$, and $S=1$, on average, for random mixtures of all mixture ratios.

TABLE I. Particle properties.

Particle name	Colors (north/south)	Mass (g)	Strength (kG)[a]	l (cm)	Magnet material
Weak	White/yellow	5.39 ± 0.11	0.22 ± 0.03	0.52	Ceramic
Strong	Blue/green	5.37 ± 0.11	0.60 ± 0.08	0.51	Nd-Fe-B
Long	Yellow/green	5.30 ± 0.23	0.54 ± 0.09	1.42	Ceramic

[a]Measured as the maximum surface field on an isolated particle.

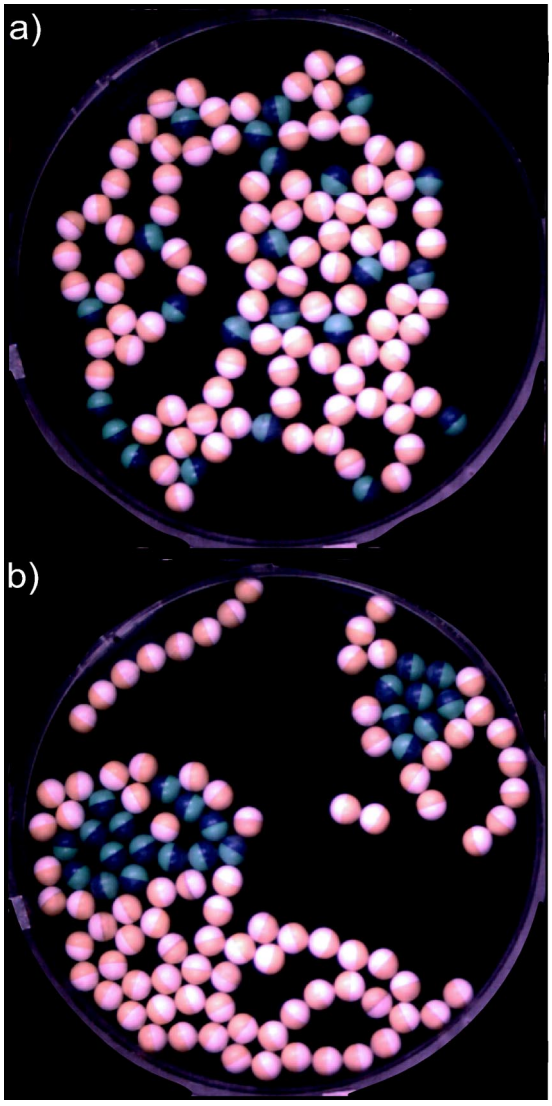

FIG. 2. (Color online) (a) The mixed initial state of a system of 88 weak (white/yellow, light/light in gray scale) and 23 strong (blue/green, dark/dark in gray scale) particles. (b) The final segregated state of the 88 weak and 23 strong particles after being shaken at 9.0*g* for 300 s. Note that there are two dense clumps of the strong particles, while the weak particles form a loose network pattern.

That $S=1$ for random mixtures of all mixture ratios, can be seen by examining the probabilities of contacts of each type:

$$p_{ij} = \begin{cases} \dfrac{N_i}{N_i + N_j - 1}, & i \neq j, \\ \dfrac{N_i - 1}{N_i + N_j - 1}, & i = j, \end{cases} \tag{2}$$

where p_{ij} is the probability that a contact associated with a particle of type i is with a particle of type j, and N_i is the total number of particles of type i in a system. So, on average,

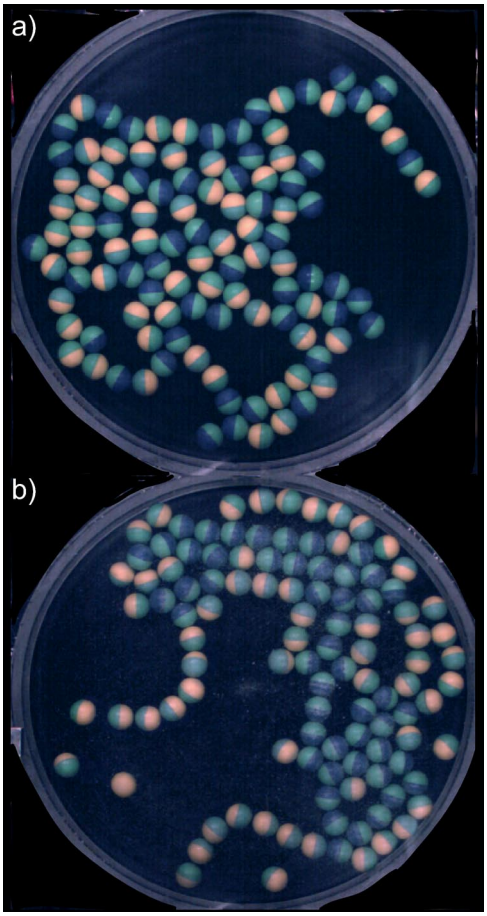

FIG. 3. (Color online) (a) The mixed initial state of a system of 51 strong (blue/green, dark/dark in gray scale) and 59 long (yellow/green, light/dark in gray scale) particles. (b) The final state of the 51 strong and 59 weak particles after being shaken at 9.6*g* for 300 s. Note that the strong particles are largely in clusters and segregated from the long particles, which form long unbranching chains.

$$C_{ij} = \kappa N_i p_{ij}, \tag{3}$$

where κ is the mean number of contacts per particle; hence, $S=1$.

Figure 4(a) is a plot of S versus time for a single trial of the 88 weak/23 strong system shown in Fig. 2. S increases from an initial value 0.86 to a final value 1.48, indicating that the system began in a state which was *supermixed* (since we intentionally placed unlike beads next to each other), i.e., more mixed than a random mixture ($S<1$) and evolved into a segregated state ($S>1$). Figure 4(b) is a plot of S versus time for a single trial of the 51 stong/59 long system in Fig. 3. S increases from an initial value 0.88 to a final value 1.39, again indicating that the system evolved from a mixed state to a segregated state. While trials with similar particle mixtures and acceleration amplitudes but differing initial conditions showed similar qualitative long time segregation behavior, the short time behavior of S versus time varied significantly in different trials.

To compare the degree of segregation of different systems after 300 s, we define a parameter S_f as the mean of S over

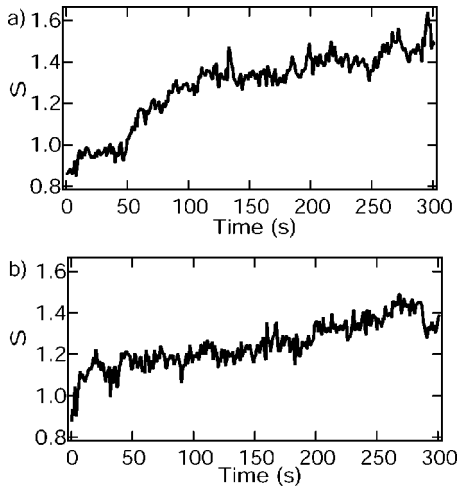

FIG. 4. (a) The segregation S versus time for the system of 88 weak and 23 strong particles shown in Fig. 2. Note that S increases significantly over time, and it is greater than 1 (the S of a randomly mixed system) at the end of the experiment. (b) S versus time for the system of 51 strong and 59 long particles shown in Fig. 3. Note that S again increases significantly over time, and it is greater than 1 at the end of the experiment.

the final 20 s of a 300-s-long experiment. Figure 5(a) is a plot of S_f versus the strong particle fraction for strong/weak systems of 111 particles driven at $9.0g$ (error bars are shown as one standard deviation of S, calculated over the final 20 s of a single experiment). S_f decreases as the fraction of strong particles is increased. Figure 5(b) is a plot of S_f versus acceleration a/g for a system of 67 weak and 44 strong particles (filled circles) and a system of 67 strong and 44 long

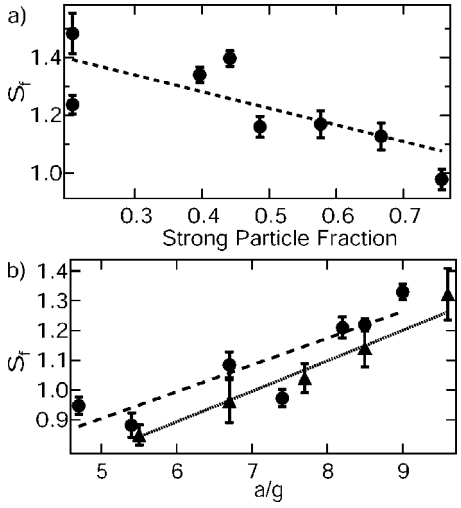

FIG. 5. (a) S_f versus the strong particle mixture fraction for strong/weak systems of 111 particles accelerated at $9.0g$. Note that S_f decreases as the number of strong particles in the mixture increases. (b) S_f versus acceleration a/g for systems of 111 particles. Mixtures of 44 strong and 67 weak particles are shown as filled circles, while mixtures of 67 strong and 44 long particles are shown as filled triangles. Note that, for both mixtures, S_f increases roughly linearly with acceleration.

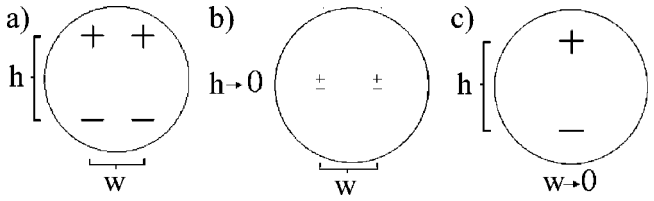

FIG. 6. (a) A schematic of our general magnetic particle model. (b) For the weak and strong particles, the model in (a) reduces to a two-point-dipole model, with the dipoles separated by a distance $w=0.31D$, where D is the particle diameter. (c) For the long particles, the model in (a) reduces to a two-charge model, with the charges separated by a distance $h=0.69D$.

particles (filled triangles). S_f increases roughly linearly with acceleration for both systems. Also, note that, in Fig. 5(b), there are several data points where $S_f<1$, indicating that, after 300 s, the systems were supermixed. This is not an indication that the systems prefer a supermixed state, rather, it is due both to the fact that the systems began in a supermixed state and to the particles' lack of mobility. The particles' lack of mobility at low accelerations is likely because the average input (driving) energy is less than the magnetic particle-particle interaction energy. In no case, for any of our systems, have we observed a significant, nontransient decrease in S in time.

IV. ENERGETIC CONSIDERATIONS

To gain insight into the cause of the observed segregation, we numerically examined a model of impenetrable spherical particles of diameter D containing four magnetic charges of equal magnitude $\pm q$, separated by distances h and w ($0 \leqslant h,w \leqslant D$), such that the charges are at the corners of a rectangle, as shown in Fig. 6(a). We vary q with h so that the dipole moment $2qh$ is constant. This model is a generalized version of the two-charge model used previously [7,20]; it reduces to the two-charge model in the limit of $w/D \rightarrow 0$. It can also be reduced to a two-point-dipole model in the limit of of $h/D \rightarrow 0$, and a single, centrally located point dipole model if $h/D \rightarrow 0$ and $w/D \rightarrow 0$.

By considering our cylindrical magnets as two uniformly charged disks of opposite sign, but equal total charge magnitude, we can then attempt to match magnetic moments of our model particles to our real particles. Using our simple two-parameter model, we match the magnetic moments of our real and model particles up to the octopole moment. The weak and strong particles, having similar shaped cores, are both modeled with two parallel point dipoles separated by a distance $w=0.31D$, as shown in Fig. 6(b). The point dipoles are approximated using $h=0.01D$ for both the weak and strong particles, with $q=11.5$ and $q=34.5$, respectively, to account for the difference in magnetic strength. The long particles are modeled with two opposite point charges of magnitude 2.0, separated by a distance of $0.69D$, as shown in Fig. 6(c).

Using our experimental particle type, position, and orientation data extracted from the images, we use our model to

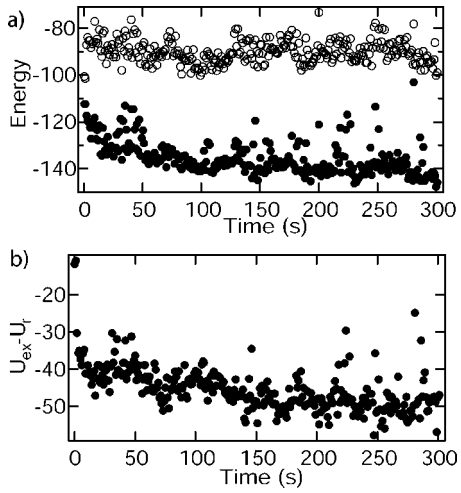

FIG. 7. (a) The magnetic energy U_{ex} versus time for the system of 88 weak and 23 strong particles shown in Fig. 2 is plotted as filled cirles. The magnetic energy of the randomly mixed state U_r is also plotted as open circles for reference. Note that U_{ex} decreases quickly within the first ten seconds, then decreases more gradually over time, while U_r remains roughly constant. (b) A plot of $U_{ex}-U_r$ versus time. $U_{ex}-U_r$ decreases steadily after the first few seconds.

approximate the total magnetostatic energy of our systems for every frame. We use the usual Coulomb energy formula $U_{ij}=q_iq_j/R_{ij}$, and sum over all inter-particle pairs of charges (excluding the energy of pairs of charges within the same particle) to obtain the energy of our experimentally observed patterns of particles, U_{ex}. As a reference, we use the magnetic energy of a randomly mixed state of the same spatial and orientational structure, which we obtain by taking the particle tracking data from the experiment, and interchanging the particle types of randomly chosen particle pairs (keeping the particle locations and dipole orientations fixed). The magnetic energy was then recalculated. This randomization and calculation process was repeated 11 times and the mean magnetic energy of the randomized system U_r was calculated for each frame. After 11 randomizations, the time average of the standard deviation of the randomized magnetic energy was 5% of U_r.

In Fig. 7(a), we have plotted U_{ex} (filled cirles) versus time for the system of 88 weak and 23 strong particles shown in Fig. 2. U_r (open circles) is also plotted in Fig. 7(a). The standard deviation of U_r is essentially constant in time at ± 5, approximately. Note that U_{ex} decreases over time, while U_r is roughly constant; also $U_{ex} \leqslant U_r$ for all time. The noticeable decrease of U_{ex} below U_r over time indicates that the decrease in U_{ex} is not an artifact of indiscriminate pattern formation, but rather a part of the segregation phenomenon. Figure 7(b) is a plot of $U_{ex}-U_r$ versus time. Note that $U_{ex}-U_r$ decreases steadily after the first few seconds. The outlying points in Figs. 7(a) and 7(b) are due to errors in particle position and orientation extraction, where false particles were detected or orientations were improperly extracted. While the observed segregation patterns tend toward states of low magnetostatic energy, it is not expected *a priori* that a driven dissipative system would arrange into a globally minimal magnetostatic energy state over long times. Rather, the observed patterns can be understood as nonequilibrium steady states.

V. CONCLUSION

Our results show that otherwise identical systems of magnetized granular particles can segregate due only to differences in their magnetic fields. Vertically vibrated monolayers of magnetic spheres can segregate both by field strength and by field shape. In binary systems of particles with differing field strength, and all other properties identical, the segregation increases with the proportion of weaker particles, and it also increases approximately linearly with acceleration over the acceleration range studied. Binary systems of particles with differing field shape and all other properties identical also show approximately linear increases in segregation as acceleration is increased over the acceleration range studied. Segregation occurs in conjunction with a decrease in magnetic energy, with the energy decrease being mostly due to the actual segregation, rather than an evolution of the spatial pattern.

The weak plastic construction of our particles prevents us from probing the behavior of our systems at higher accelerations; however, it seems likely that at high accelerations, the input vibration energy would exceed the magnetic interaction energy, and systems such as ours would remix. While we expect the qualitative behavior of larger systems to be similar, the small size of the systems we studied makes it difficult to obtain high-quality quantitative statistical results. Possible future work includes studies of larger binary systems of magnetic particles, and using more sturdily constructed particles that allow the investigation of higher accelerations.

ACKNOWLEDGMENTS

This work was supported by ONR (Physics), NSF (Grants No. 0243824 and No. Physics098632), and NASA Grant No. NAG32736.

[1] J. Ottino and D. Khakhar, Annu. Rev. Fluid Mech. **32**, 55 (2000).
[2] M. Newey, J. Ozik, S. M. van der Meer, E. Ott, and W. Losert, Europhys. Lett. **66**, 205 (2004).
[3] H. Li and J. J. McCarthy, Phys. Rev. Lett. **90**, 184301 (2003).
[4] A. Samadani and A. Kudrolli, Phys. Rev. E **64**, 051301 (2001).
[5] N. Lecocq and N. Vandewalle, Fractals **11**, 259 (2003).
[6] H. A. Makse, S. Havlin, P. R. King, and H. E. Stanley, Nature (London) **386**, 379 (1997).

[7] J. Stambaugh, D. P. Lathrop, E. Ott, and W. Losert, Phys. Rev. E **68**, 026207 (2003).
[8] D. L. Blair and A. Kudrolli, Phys. Rev. E **67**, 021302 (2003).
[9] K. De'Bell, A. B. MacIsaac, and J. P. Whitehead, Rev. Mod. Phys. **72**, 225 (2000).
[10] M. Golosovsky, Y. Saado, and D. Davidov, Appl. Phys. Lett. **75**, 4168 (1999).
[11] W. Wen, L. Zhang, and P. Sheng, Phys. Rev. Lett. **85**, 5464 (2000).
[12] G. Helgesen and A. T. Skjeltorp, J. Appl. Phys. **69**, 8277 (1991).
[13] W. Wen, F. Kun, K. F. Pál, D. W. Zheng, and K. N. Tu, Phys. Rev. E **59**, R4758 (1999).
[14] A. T. Skjeltorp, Phys. Rev. Lett. **51**, 2306 (1983).
[15] A. Wachowiak, J. Wiebe, M. Bode, O. Pietzsch, M. Morgenstern, and R. Wiesendanger, Science **298**, 577 (2002).
[16] J. J. Weis, Mol. Phys. **100**, 579 (2002).
[17] J. J. Weis, Mol. Phys. **93**, 361 (1998).
[18] K. De'Bell, A. B. MacIsaac, I. N. Booth, and J. P. Whitehead, Phys. Rev. B **55**, 15 108 (1997).
[19] B. Trpišová and J. A. Brown, Int. J. Mod. Phys. B **12**, (1998).
[20] K.-P. Schneider and J. Keller, Chem. Phys. Lett. **275**, 63 (1997).
[21] J. S. Olafsen and J. S. Urbach, Phys. Rev. Lett. **81**, 4369 (1998).
[22] W. Losert, D. G. W. Cooper, and J. P. Gollub, Phys. Rev. E **59**, 5855 (1999).
[23] E. Ben-Naim, Z. A. Daya, P. Vorobieff, and R. E. Ecke, Phys. Rev. Lett. **86**, 1414 (2001).